J|A|C|S ARTICLES

Published on Web 04/30/2009

High Hydrogen Storage Capacity of Porous Carbons Prepared by Using Activated Carbon

Huanlei Wang, Qiuming Gao,* and Juan Hu

State Key Laboratory of High Performance Ceramics and Superfine Microstructures, Graduate School, Shanghai Institute of Ceramics, Chinese Academy of Sciences, 1295 Dingxi Road, Shanghai 200050, People's Republic of China

Received October 23, 2008; E-mail: qmgao@mail.sic.ac.cn

Abstract: A kind of activated carbon with further carbon dioxide and potassium hydroxide activations for hydrogen storage was investigated. The carbon dioxide and potassium hydroxide activations have apparently different effects on the pore structures and textures of the activated carbon which closely associated with the hydrogen storage properties. The potassium hydroxide activation can remarkably donate microporosity to the frameworks of the activated carbon. One of the resultant porous carbons exhibited a high surface area of up to 3190 $m^2 g^{-1}$ and large gravimetric hydrogen uptake capacity of 7.08 wt % at 77 K and 20 bar, which is one of the largest data reported for the porous carbon materials. This result suggests that the porous carbon with large amounts of active sites, high surface area, and high micropore volume related to optimum pore size could achieve high gravimetric hydrogen storage.

Introduction

To resolve the present energy and environmental problems caused by the depleting of fossil fuels, hydrogen is gaining increasing attention as a solution to these problems, mainly due to its abundance, high chemical energy, and pollution-free burning.[1] However, hydrogen storage is the "bottleneck" that holds up the realization of on-board application using hydrogen as energy carrier. There are essentially several ways to store hydrogen, including liquefaction, compressed gas, metal hydrides, chemical hydrides, and porous adsorbents. Unfortunately, none of these technologies are good enough to satisfy all the criteria of size, efficiency, cost, kinetics, and safety required for the transportation application, even though each way possesses desirable characteristics in certain areas.[1−3] Among them, porous carbon materials as a candidate for hydrogen storage attracted extensive attention as a result of the advantages associated with its light weight, fast kinetics, complete reversibility, low cost, and high surface area.[4,5] In general, high surface area and micropore volume are essential for enhancing the hydrogen storage capacity.[6−8] Hence, tailoring pore structures and textures of the porous carbon materials for hydrogen storage is an urgent matter.

Recently, template carbonization was applied to receive porous carbons with tunable structures and textures through the selection of templates, carbon sources, infiltration methods, and filling degree of the carbon precursor in the pore system of templates.[9] The hydrogen test of zeolite-templated carbons demonstrated that the porous carbon materials can be promising candidates for hydrogen storage.[6] However, the template technique is costly and requires complicated processes, which limits its industrial application. Another developed technique to produce microporous carbons with tunable pore size distributions is the carbide-derived carbon (CDC) technique.[10,11] The CDC can be obtained through the selective reaction of carbides with halogen gases and the pore structures of CDC can be easily controlled by the parameters of the synthesis process. The TiC-derived carbon exhibited the highest hydrogen storage capacity at 77 K and 1 bar.[12,13] However, the surface areas and micropore volumes of the CDCs could not exceed that of the zeolite-templated carbons, which limited their application in the hydrogen storage. It is noteworthy that one of the porous carbon materials with a simple preparation process and long history is activated carbon, but the surface areas of most activated carbons are not high enough and their pore size distributions are broad, which are not beneficial for the hydrogen storage. The methodology used for preparation of activated carbon can be successively applied to further control the microstructure and donate microporosity to the frameworks of the carbons. As is generally organized, there are typical two kinds of activation procedures, namely, physical and chemical activations.[14] The physical activation involves gasification of the carbon materials

(1) Schlapbach, L.; Züttel, A. *Nature* **2001**, *414*, 353.
(2) Zhao, X. B.; Xiao, B.; Fletcher, A. J.; Thomas, K. M. *J. Phys. Chem. B* **2005**, *109*, 8880.
(3) Qu, D. *Chem.—Eur. J.* **2008**, *14*, 1040.
(4) Hirscher, M.; Panella, B. *J. Alloys Compd.* **2005**, *404−406*, 399.
(5) Hu, Q.; Lu, Y.; Meisner, G. P. *J. Phys. Chem. C* **2008**, *112*, 1516.
(6) Yang, Z.; Xia, Y.; Mokaya, R. *J. Am. Chem. Soc.* **2007**, *129*, 1673.
(7) Pacula, A.; Mokaya, R. *J. Phys. Chem. C* **2008**, *112*, 2764.
(8) Xu, W. C.; Takahashi, K.; Matsuo, Y.; Hattori, Y.; Kumagai, M.; Ishiyama, S.; Kaneko, K.; Iijima, S. *Int. J. Hydrogen Energy* **2007**, *32*, 2504.
(9) Lu, A. H.; Schüth, F. *Adv. Mater.* **2006**, *18*, 1793.
(10) Gogotsi, Y.; Nikitin, A.; Ye, H.; Zhou, W.; Fischer, J. E.; Yi, B.; Foley, H. C.; Barsoum, M. W. *Nat. Mater.* **2003**, *2*, 591.
(11) Chmiola, J.; Yushin, G.; Gogotsi, Y.; Portet, C.; Simon, P.; Taberna, P. L. *Science* **2006**, *313*, 1760.
(12) Gogotsi, Y.; Dash, R. K.; Yushin, G.; Yildirim, T.; Laudisio, G.; Fischer, J. E. *J. Am. Chem. Soc.* **2005**, *127*, 16006.
(13) Yushin, G.; Dash, R.; Jagiello, J.; Fischer, J. E.; Gogotsi, Y. *Adv. Funct. Mater.* **2006**, *16*, 2288.
(14) Cardoso, B.; Mestre, A. S.; Carvalho, A. P.; Pires, J. *Ind. Eng. Chem. Res.* **2008**, *47*, 5841.

10.1021/ja8083225 CCC: $40.75

Table 1. Textural Parameters of the Porous Carbon Materials

sample	S_{BET}[a] ($m^2\ g^{-1}$)	V_t[b] ($cm^3\ g^{-1}$)	V_{meso}[c] ($cm^3\ g^{-1}$)	V_{micro}[d] ($cm^3\ g^{-1}$)	$V_{<1nm}$[e] ($cm^3\ g^{-1}$)	V_{micro}/V_t (%)	D_{BJH}[f](nm)	D_{HK}[g] (nm)	carbon yields (%)	packing density ($g\ cm^{-3}$)
AC	1585	1.44	0.85	0.59	0.17	41	3.9	1.3	−	0.80
AC-C2	1488	1.22	0.62	0.60	0.21	49	3.6	1.1	62	0.62
AC-C4	1308	1.10	0.58	0.52	0.19	47	3.6	1.1	49	0.69
AC-K3	2009	1.00	0.18	0.82	0.69	82	2.8	0.59	53	0.67
AC-K5	3190	1.69	0.60	1.09	0.79	64	2.5	0.67	43	0.61

[a] The specific surface area (S_{BET}) was calculated by the Brunauer−Emmet−Teller (BET) method in the relative pressure range of 0.02−0.25. [b] V_t represented the total pore volume. [c] The mesopore volume (V_{meso}) was obtained by subtracting the microporous volume from total pore volume. [d] The micropore volume (V_{micro}) was determined by applying Dubinin−Radushkevich (DR) analysis. [e] The volume of pores smaller than 1 nm ($V_{<1nm}$) was determined by the cumulative pore volume using the Horvath−Kawazoe (HK) method. [f] D_{BJH} stands for the Barrett−Joyner−Halenda (BJH) desorption average pore width. [g] D_{HK} represents the median micropore size by the HK method.

in the presence of suitable oxidizing gasifying agents, such as CO_2 and steam.[15] In the chemical activation, the prominent reaction occurring between the chemical agents such as KOH and the carbon materials is mostly as follows:[16]

$$6KOH + 2C \leftrightarrow 2K + 3H_2 + 2K_2CO_3 \quad (1)$$

The carbon framework is etched to generate pores, because of oxidation of the carbon into carbonate ion and intercalation of the potassium compounds.[17] On the other hand, the production of CO_2 from the decomposition of K_2CO_3 at temperatures above 700 °C can contribute to further porosity development through the carbon gasification.[18] The chemical activation presents several advantages compared to the physical activation, such as lower processing temperature, shorter reaction time, and higher microporosity, but it faces the disadvantage of having to thoroughly wash away impurities generated during the activation process.[19,20]

Here, the target of activation is to enhance the microporosity and amounts of the active sites that may be beneficial for the hydrogen storage. Both physical and chemical activations were performed in our study. This paper focuses not only on the different impact of CO_2 and KOH activations on the pore structures and textures of the activated carbon but also on the relationship between the porous structures and hydrogen storage properties, which may help to clarify the hydrogen adsorption mechanism and increase our sight for designing suitable carbon-based hydrogen storage systems.

Experimental Section

Synthesis. A selected activated carbon (abbreviated as AC, chemically pure, Shanghai Dahe Chemical Reagent Ltd.) was chosen as an initial sample.[21] During the CO_2 activation, the as-received activated carbon was first placed in the center of a quartz tube in a tube furnace and then heated to the activation temperature of 1223 K with a heating rate of 5 K min^{-1} under nitrogen. When the furnace reached the desired temperature, a CO_2 gas stream (10 mL min^{-1}) was introduced into the tube furnace. Finally, the sample was cooled down under nitrogen. The resultant samples were denoted as AC-C2 and AC-C4 after the treatments in the gas stream of CO_2 at 1223 K for 2 and 4 h, respectively. The KOH activation was performed by heating the physical mixture of the activated carbon and KOH under argon atmosphere. The mixture of the activated carbon and KOH was placed in the center of an alumina tube in a tube furnace and then heated to the activation temperature of 1023 K with a heating rate of 1.25 K min^{-1} under argon, followed by a "heat soak" time of 1 h at this temperature. Finally, the mixture was recovered and washed three times with 3 M hydrochloric acid at room temperature and then with sufficient deionized water. The resultant sample was then dried at 373 K for 12 h. The obtained samples were denoted as AC-K3 and AC-K5, in which K3 and K5 denote KOH/AC mass ratios of 3:1 and 5:1. The yields of the carbons after the activations are listed in Table 1.

Characterization. Powder X-ray diffraction (XRD) pattern analysis was performed on a Rigaku D/MAX-2200 diffraction using Ni-filtered Cu Kα radiation (λ = 1.5418 Å). High-resolution transmission electron microscopy (HRTEM) images were measured on a JEOL (JEM-2100F) microscope operating at 200 kV. The specific surface area and pore structure were investigated with a Micrometrics ASAP 2020 system using nitrogen as the adsorbate at 77 K. Prior to determination of the isotherm, the samples were degassed below 1.33 Pa at 363 K for 1 h and heated (10 K min^{-1}) to 623 K for at least 6 h. Hydrogen uptake measurements were performed by volumetric methods (Micrometrics ASAP 2020) under the pressure range of 0−1 bar at 77 K and gravimetric methods (Rubotherm) under 1−20 bar at 77 K (see the Supporting Information).[22] The packing densities (Table 1) of the carbon materials were evaluated by pressing a given amount of sample in a mold at a pressure of 10 MPa using a cylindrical rod.[23,24] The measurement of the height of the rod with the mold empty and with sample allows the determination of the volume of the carbon materials and then the packing density. The amount of the sample used was about 0.3−0.6 g, and the measurements were repeated three times with an error smaller than 3%.

Results and Discussion

Structure Analysis. XRD patterns of the activated carbon and porous carbon materials after the CO_2 and KOH activations are shown in Figure 1. As a measure of the number of carbon sheets arranged as single layers, Dahn et al.[25] used the empirical parameter (R), which is defined as the ratio of height of the (002) Bragg peak to the background, and the values of R for each sample are also shown in Figure 1. It has been demonstrated that the R values decrease as the single layer contents in the carbon increase;[3] e.g., a larger R value indicates a higher degree of the graphitization, which suggests a larger concentration of the parallel single layers in the carbon materials. The R values of AC-C2 and AC-C4 (R = 2.2 and 2.0, respectively)

(15) Chang, C. F.; Chang, C. Y.; Tsai, W. T. *J. Colloid Interface Sci.* **2000**, *232*, 45.
(16) Lillo-Ródenas, M. A.; Juan-Juan, J.; Cazorla-Amorós, D.; Linares-Solano, A. *Carbon* **2004**, *42*, 1371.
(17) Lozano-Castelló, D.; Calo, J. M.; Cazorla-Amorós, D.; Linares-Solano, A. *Carbon* **2007**, *45*, 2529.
(18) Teng, H. S.; Hsu, L. Y. *Ind. Eng. Chem. Res.* **1999**, *38*, 2947.
(19) Choi, M.; Ryoo, R. *J. Mater. Chem.* **2007**, *17*, 4204.
(20) Lillo-Ródenas, M. A.; Cazorla-Amorós, D.; Linares-Solano, A. *Carbon* **2003**, *41*, 267.
(21) Hu, J.; Gao, Q.; Wu, Y.; Song, S. *Int. J. Hydrogen Energy* **2007**, *32*, 1943.
(22) Fang, Q. R.; Zhu, G. S.; Jin, Z.; Ji, Y. Y.; Ye, J. W.; Xue, M.; Yang, H.; Wang, Y.; Qiu, S. L. *Angew. Chem., Int. Ed.* **2007**, *46*, 6638.
(23) de la Casa-Lillo, M. A.; Lamari-Darkrim, F.; Cazorla-Amorós, D.; Linares-Solano, A. *J. Phys. Chem. B* **2002**, *106*, 10930.
(24) Jordá-Beneyto, M.; Lozano-Castelló, D.; Suárez-García, F.; Cazorla-Amorós, D.; Linares-Solano, A. *Microporous Mesoporous Mater.* **2008**, *112*, 235.
(25) Liu, Y.; Xue, J. X.; Zheng, T.; Dahn, J. R. *Carbon* **1996**, *34*, 193.

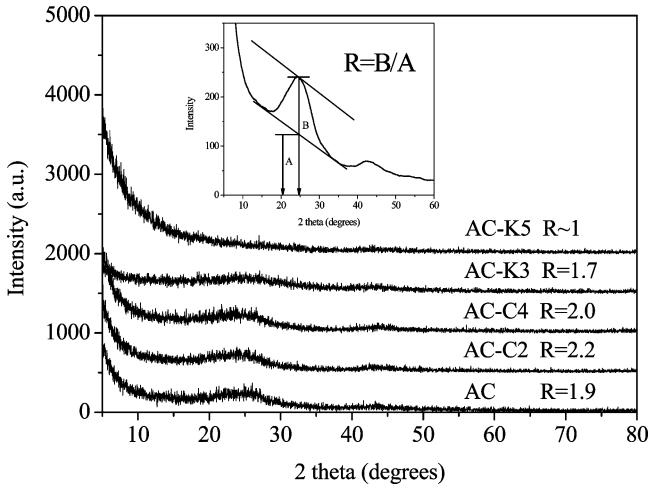

Figure 1. XRD patterns of the activated carbon materials with the CO_2 and KOH activations. The inset is a sketch map for the calculation of the *R* values.

are a little larger than that of AC ($R = 1.9$), because a relatively higher activation temperature during the CO_2 gas flow may lead to some edge orientation and reduce the concentration of nonparallel single layers. Thus, the CO_2 activation could result in a little higher degree of graphitization of the structure. As to AC-K3 and AC-K5, the *R* values decreased after the KOH activations. It is noteworthy that the *R* value of sample AC-K5 is close to 1, which is due to almost randomly distributed graphene sheets in the structure. As a result, the KOH activation may lead to a breakdown of aligned structural domains in the carbon matrix due to the intercalation of the potassium compounds.[25,26]

HRTEM images are shown in Figure 2. It is clear that AC-C2 has apparent oriented multilayer domains and possesses graphene sheets stacking in parallel (Figure 2b). Both samples AC and AC-C2 have more graphene sheets stacking in parallel than AC-K5 (Figure 2c,d). For sample AC-K5, more disordered graphene layer domains were observed, and the graphene layer domains became shorter after the KOH activation, in accordance with the XRD analysis.

Porosity Analysis. Nitrogen adsorption and desorption isotherms for AC, AC-C2, and AC-C4 are shown in Figure 3a. For comparison, the textural parameters are listed in Table 1. Type-IV isotherms could be found for all samples. Hysteresis loop character may be observed for AC, AC-C2, and AC-C4 samples in a wide relative pressure range of 0.4−0.9, which are associated with the capillary condensations taking place in the mesopores. Generally speaking, the CO_2 activation not only involves the reaction between the carbon and CO_2, resulting in the removal of carbon atoms, but also plays an important role in enhancing the microporosity, leading to a higher specific surface area.[27] However, it is depressing to note that the specific surface area of the activated carbon materials decreased gradually from 1585 $m^2\ g^{-1}$ for AC to 1488 $m^2\ g^{-1}$ for AC-C2 to 1308 $m^2\ g^{-1}$ for AC-C4 along with the increase of the activation time. Moreover, the change of the total pore volume is consistent with that of the specific surface area, which may indicate that the destruction of high porosity is more pronounced during the CO_2 activation. The percentages of micropore volume in total pore volume of the carbon materials after the CO_2 activation (49% for AC-C2 and 47% for AC-C4) are higher than that of the initial activated carbon (41%), which implies that gasification by CO_2 develops certain microporosity. The percentage of micropore volume in total pore volume of AC-C4 is a little lower than that of AC-C2, indicating that longer activation time had a somewhat negative effect on creating the micropores. The pore sizes analyzed by the BJH and HK methods show that the primary mesopore and micropore sizes were reduced from 3.9 and 1.3 nm for AC to 3.6 and 1.1 nm for either AC-C2 or AC-C4. The decreases of pore size of the activated samples with the CO_2 activation are in accordance with the increase of the percentage of micropore volume.

Table 1 also compiles the details of the textural parameters of AC-K3 and AC-K5. For clarity, the corresponding nitrogen sorption isotherms are shown in Figure 3b. The nitrogen sorption isotherms are typical type-I for AC-K3 and mixed type-I and -IV for AC-K5 with well-defined plateaus, indicating the apparent micropore character of the carbon materials after the KOH activation. Moreover, the broadening of the knee in the relatively low pressure range for AC-K5 exhibited small mesopores developed upon increasing KOH/AC mass ratio to 5:1. As shown in Table 1, the specific surface area of the carbon materials dramatically increased after the KOH activation. It is worth emphasizing that AC-K5 can achieve a high surface area of 3190 $m^2\ g^{-1}$, which is as high as the theoretical surface area of a double-sided separated graphene sheet (2965 $m^2\ g^{-1}$).[28] Compared to the initial activated carbon, both AC-K3 and AC-K5 exhibited higher micropore volumes when treated by the KOH activation. The micropore volumes gradually increased from 0.59 $cm^3\ g^{-1}$ for AC to 0.82 $cm^3\ g^{-1}$ for AC-K3 to 1.09 $cm^3\ g^{-1}$ for AC-K5. Moreover, the percentage of micropore volume for AC-K3 can reach 82% after the KOH activation, which is twice that of AC. However, when the KOH/AC mass ratio was increased to 5:1, the percentage of micropore volume decreased to 64% and small mesopores developed as the result of the widening of the pre-existing micropores. The micropore sizes of AC-K3 and AC-K5 are centered at about 0.59 and 0.67 nm, respectively, analyzed by the HK method.

Hydrogen Storage at 77 K and 1 bar. Hydrogen adsorption isotherms of those carbon materials from 0−1 bar at 77 K by the volumetric method are shown in Figure 4. The capacity with a linear dependence on surface area is expected.[29,30] It is found that both AC-K5 and AC-K3 with higher surface areas have larger hydrogen storage capacities (2.49 wt % for AC-K5 and 2.23 wt % for AC-K3) than that of AC, AC-C2, and AC-C4 (see Table 1). Further detailed studies show that the hydrogen storage capacities of AC-C2 (1.70 wt %) and AC-C4 (1.27 wt %) were also higher than that of AC (1.23 wt %), even though the surface areas were decreased for either AC-C2 or AC-C4. At the same time, several investigations revealed that linear relationships could be observed between the hydrogen uptake capacity and micropore volume or volume of pores smaller than 1 nm.[12,31] Thus, the pore volumes of mesopores (≥2 nm), micropores (<2 nm), and ultrafine micropores (<1 nm) in comparison with the hydrogen uptake capacities as a function

(26) Subramanian, V.; Luo, C.; Stephan, A. M.; Nahm, K. S.; Wei, B. *J. Phys. Chem. C* **2007**, *111*, 7527.
(27) Xia, K.; Gao, Q.; Song, S.; Wu, C.; Jiang, J.; Hu, J.; Gao, L. *Int. J. Hydrogen Energy* **2008**, *33*, 116.
(28) Chae, H. K.; Siberio-Perez, D. Y.; Kim, J.; Go, Y.; Eddaoudi, M.; Matzger, A. J.; ÓKeeffe, M.; Yaghi, O. M. *Nature* **2004**, *427*, 523.
(29) Pang, J. B.; Hampsey, J. E.; Wu, Z. W.; Hu, Q. Y.; Lu, Y. F. *Appl. Phys. Lett.* **2004**, *85*, 4887.
(30) Yang, Z.; Xia, Y.; Sun, X.; Mokaya, R. *J. Phys. Chem. B* **2006**, *110*, 18424.
(31) Xia, K.; Gao, Q.; Wu, C.; Song, S.; Ruan, M. *Carbon* **2007**, *45*, 1989.

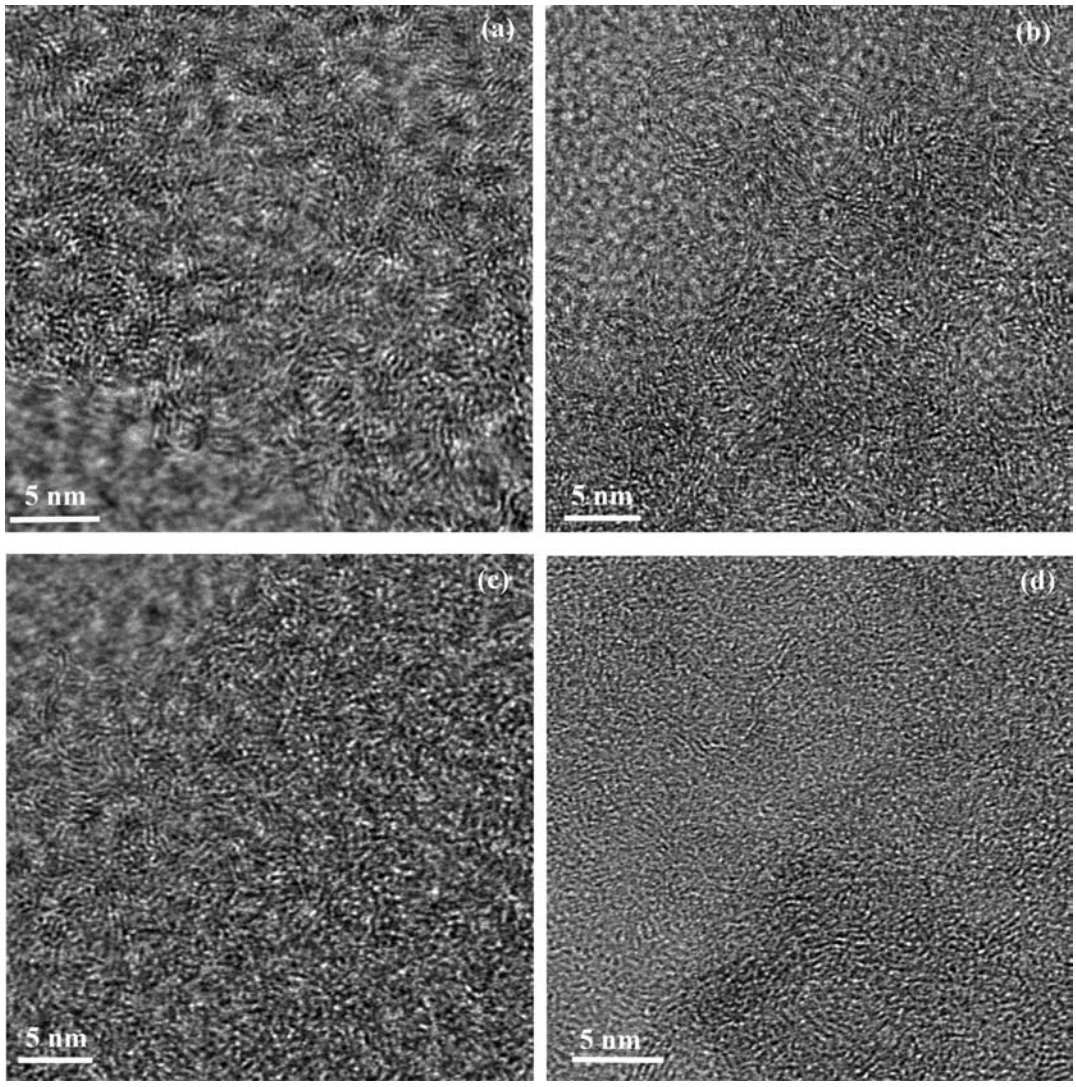

Figure 2. HRTEM images of AC (a), AC-C2 (b), and AC-K5 (c and d) samples.

of different samples are shown in Figure 5. A similar tendency could be observed between the hydrogen uptake capacity and the volume of pores smaller than 1 nm. So, the $V_{<1nm}$ of AC, AC-C2, and AC-C4 has a close relationship with the hydrogen storages at 77 K and 1 bar. Besides, the V_{micro}/V_t of AC (41%) is lower than that of either AC-C2 (49%) or AC-C4 (47%), and their hydrogen storage capacities follow the same sequence (AC, 1.23 wt %; AC-C2, 1.70 wt %; and AC-C4, 1.27 wt %); thus, we may deduce that the porous carbon material with higher micropore volume proportion will have relatively larger hydrogen uptake. In the case of AC-K3 and AC-K5, AC-K5 has an apparently higher $V_{<1nm}$ (0.79 $cm^3\ g^{-1}$) than that of AC-K3 (0.69 $cm^3\ g^{-1}$). Correspondingly, AC-K5 has a higher hydrogen storage capacity (2.49 wt % at 77 K and 1 bar) than that of AC-K3 (2.23 wt %), even though their V_{micro}/V_t values are in a reverse sequence. So, $V_{<1nm}$ value of porous carbon may be more important than V_{micro}/V_t for the hydrogen storage at 77 K and 1 bar.

The normalized hydrogen uptakes are shown in Figure 6.[32] We can find that AC-K3 has the lowest pressure at which half of the total adsorption capacity at 1 bar is adsorbed ($P_{1/2}$), and this confirms the strong interaction between hydrogen and the pores of AC-K3. The median micropore size of AC-K3 is 0.59 nm, and these very small pores lead to a strong binding affinity due to the increased van der Waals contact area. The diameter is close to the reported optimum pore size of about 0.6−0.7 nm for hydrogen storage,[13,31,33] which is believed to be able to hold two layers of adsorbed hydrogen. Additionally, the developed microporosity with the high V_{micro}/V_t (82%) for AC-K3 could provide strong van der Waals interactions. Although the $P_{1/2}$ values of AC and AC-K5 are almost the same, the hydrogen uptake of AC-K5 (2.49 wt %) is about double that of AC (1.23 wt %), which may be due to its ultrahigh surface area (3190 $m^2\ g^{-1}$), suitable micropore size (about 0.67 nm), and high V_{micro}/V_t (64%). As a result, there may exists a synergistic effect on the hydrogen storage of porous carbon materials. Generally, the porous carbons with high surface area and developed microporosity could achieve high hydrogen storage at 77 K and 1 bar.

Hydrogen Storage at 77 K and 20 bar. The hydrogen uptake, measured by the gravimetric method at 77 K over the pressure range 1−20 bar, is shown in Figure 7. To verify our hydrogen uptake measurements, we compared our data with that of a well-

(32) Jhung, S. H.; Yoon, J. W.; Lee, J. S.; Chang, J. S. *Chem.—Eur. J.* **2007**, *13*, 6502.

(33) Texier-Mandoki, N.; Dentzer, J.; Piquero, T.; Saadallah, S.; David, P.; Vix-Guterl, C. *Carbon* **2004**, *42*, 2744.

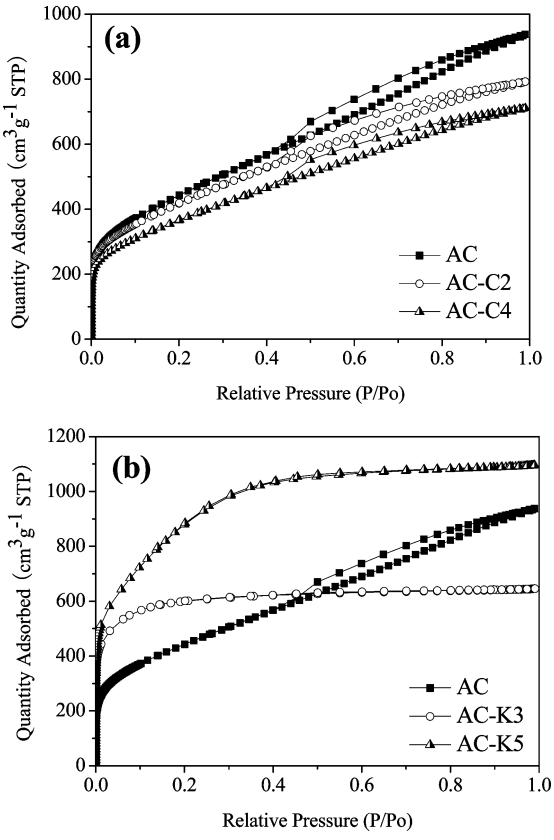

Figure 3. Nitrogen adsorption−desorption isotherms of the porous carbon materials with the CO_2 (a) and KOH activations (b).

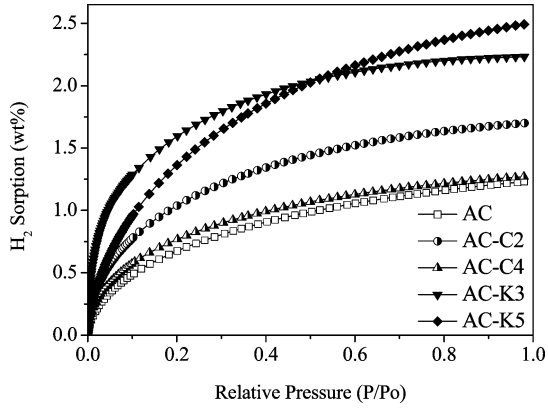

Figure 4. Hydrogen adsorption isotherms of the porous carbon materials from 0 to 1 bar at 77 K by the volumetric method.

known commercial activated carbon (G212, provided by PICA, Vierzon, France). The hydrogen uptakes of G212 were 1.80 wt % at 1 bar and 3.88 wt % at 20 bar (Figure 7), which are close to the value obtained by Mokaya's group (3.96 wt % at 77 K and 20 bar).[6] It is worth emphasizing that the hydrogen adsorption capacity has a better linear relationship with the surface area at higher pressure (20 bar) than that at lower pressure (1 bar) (Figure 8a), because the available adsorption sites were more fully saturated at 20 bar. According to the literature,[3] the active sites for hydrogen storage on the carbon materials are mainly the oriented edges of microdomains related to the *R* values. The larger the *R* values are, the higher the edge orientation will be. From Figure 9, it can be seen that the hydrogen uptake capacity per unit surface area increased along with the increase of the *R* values, indicating that higher edge orientation results in an increased hydrogen uptake

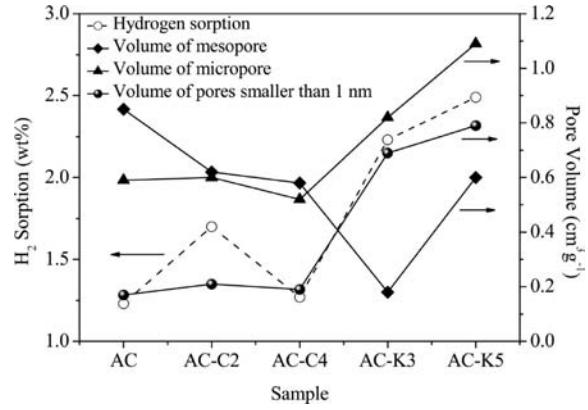

Figure 5. Pore volumes in comparison with the hydrogen sorption at 77 K and 1 bar as a function of the porous carbon materials.

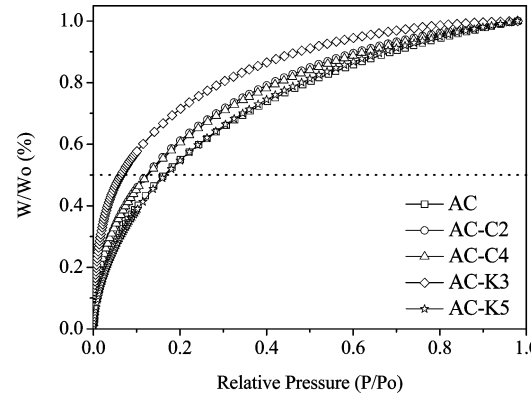

Figure 6. Hydrogen adsorption isotherms normalized to the adsorption capacity from 0−1 bar over different porous carbon materials.

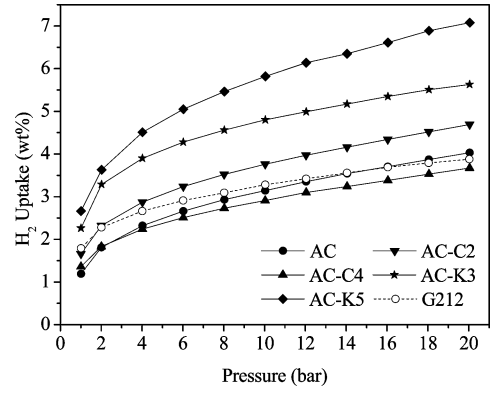

Figure 7. Hydrogen uptake curves of the porous carbon materials by the gravimetric method at 77 K over the pressure range 1−20 bar.

per square meter. Thus, orientation of the graphene sheets may also play an important role in the hydrogen uptake at 77 K and 20 bar and larger *R* values lead to higher active sites per surface area. Moreover, the micropores could provide the carbon materials a larger adsorption potential and a stronger van der Waals interaction with the hydrogen molecules. Correspondingly, the micropores may have an essential relationship with hydrogen storage at 77 K and 20 bar. An approximately linear relationship was observed between the hydrogen uptake capacity and micropore volume at 77 K and 20 bar (Figure 8b). The result indicates that the pore with diameter between 1 and 2 nm may contribute more at 20 bar than that at 1 bar, which could result in more candidates for porous carbon materials having the potential of high hydrogen storage capacity

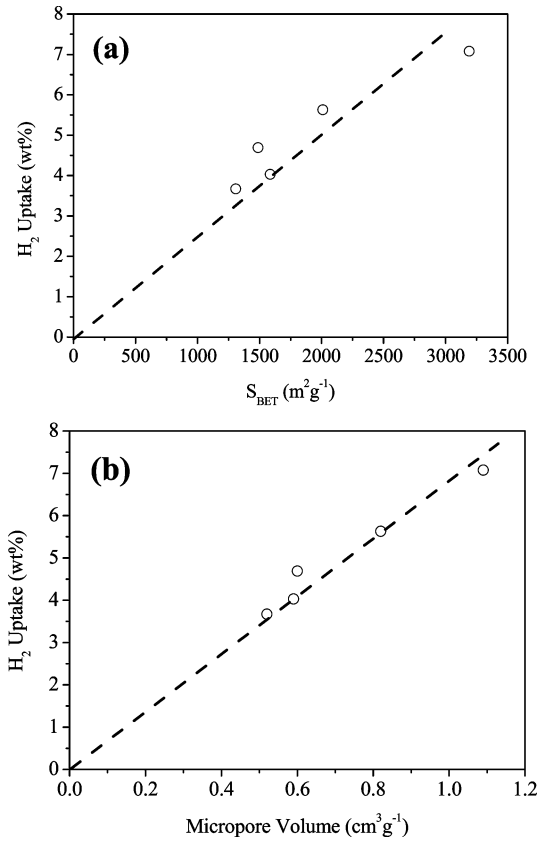

Figure 8. Relationships between the hydrogen uptake and surface area (a) or micropore volume (b).

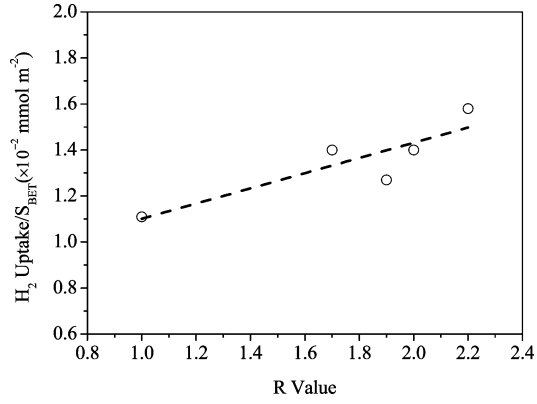

Figure 9. Hydrogen uptake capacity per unit surface area versus the *R* values.

at 77 K and 20 bar. Thus, at higher pressures, not only pore characters but also active sites have important contributions to the hydrogen storage. It should be mentioned that the resultant activated carbon AC-K5 displayed a hydrogen uptake capacity of 7.08 wt % at 77 K and 20 bar, which is one of the largest values ever reported for the porous carbon materials (see Table 2). The corresponding volumetric hydrogen storage of 43.2 g L^{-1} for AC-K5 was also obtained by multiplication of the packing density and gravimetric hydrogen storage value, and giving the hydrogen storage capacity on a volumetric basis is important from an application point of view. Further increasing the surface area, V_{micro} (or V_{micro}/V_t ratio, microporosity), and the number of active sites would be the focus for the porous carbon material in order to have a higher capacity of hydrogen storage at 77 K and 20 bar.

Table 2. Hydrogen Uptake Capacities at 77 K for the Selected Porous Carbons and Templated Carbons (TC)

sample	S_{BET} (m^2 g^{-1})	H_2 uptake (wt %)	ref
AC-K3	2009	5.63 (20 bar)	this work
AC-K5	3190	7.08 (20 bar)	this work
AX-21 (AC)	2800	4.6 (10 bar)	34
KUA-6 (AC)	3808	5.6 (40 bar)	35
Maxsorb-3000 (AC)	3178	5.2 (40 bar)	35
CB850h (TC)	3150	6.9 (20 bar)	6
TC	2535	5.3 (20 bar)	7

Conclusions

In summary, physical and chemical activations for the activated carbon were investigated. Compared to CO_2 activation, KOH activation can remarkably change pore structures of the activated carbon. The nitrogen sorption isotherms changed from type-IV (AC) to type-I (AC-K3) or mixed type-I and -IV (AC-K5), the specific surface areas increased greatly from 1585 m^2 g^{-1} (AC) to 2009 m^2 g^{-1} (AC-K3) to 3190 m^2 g^{-1} (AC-K5), the microporosity noticeably donated to the carbon frameworks with the V_{micro}/V_t of 82% for AC-K3 and 64% for AC-K5, and narrow pore size distributions were obtained after the KOH activation. The KOH activation could lead to a low degree of graphitization with more disordered graphene layer domains in the structure of the porous carbons. The CO_2 activation may result in some improvement of the microporosity and a small high degree of graphitization with apparent oriented multilayer domains and graphene sheets stacking in parallel in the structure of the porous carbons.

Cryogenic hydrogen adsorption capacities (77 K) were determined at 1 and 20 bar. A better linear relationship was observed between hydrogen adsorption capacity and surface area at higher pressure (20 bar) than that at lower pressure (1 bar), because the available adsorption sites were more fully saturated at the high pressure. The active sites for hydrogen storage on porous carbon materials are mainly the edge orientation of microdomains related to the *R* values, which could be adjusted by the CO_2 or KOH activation. Higher edge orientation results in an increased hydrogen uptake per square meter. The improved linear relationship between the hydrogen uptake capacity and micropore volume indicates that the pore with diameter between 1 and 2 nm contributed more at 20 bar than that at 1 bar, which may result in more candidates of porous carbon materials having the potential of high hydrogen storage capacity at 77 K and 20 bar.

An enhanced hydrogen uptake of 7.08 wt % was successfully achieved for the as-obtained porous carbon AC-K5 at 77 K and 20 bar. The results indicate that the second activated carbons are promising materials for hydrogen storage, and higher gravimetric hydrogen uptake could be obtained if one can improve the microporosity with high surface area related to optimum pore size distribution and increase the number of active sites. Furthermore, the activated carbons may also possess wide application fields ranging from catalyst to energy conversion.

(34) Chen, F.; Liang, J.; Zhao, J.; Tao, Z.; Chen, J. *Chem. Mater.* **2008**, *20*, 1889.
(35) Jordá-Beneyto, M.; Suárez-García, F.; Lozano-Castelló, D.; Cazorla-Amorós, D.; Linares-Solano, A. *Carbon* **2007**, *45*, 293.

Acknowledgment. We thank the Chinese National Science Foundation (No. U0734002) and Shanghai Nanotechnology Promotion Center (No. 0652nm025 and 0852nm0500) for financial support.

Supporting Information Available: Procedures for high-pressure hydrogen storage measurement, hydrogen storage of the commercially available activated carbon G212, and repeated hydrogen uptake measurements of the sample AC-K5. This material is available free of charge via the Internet at http://pubs.acs.org.

JA8083225